JACS
JOURNAL OF THE AMERICAN CHEMICAL SOCIETY
Article
Cite This: J. Am. Chem. Soc. 2018, 140, 11855−11862
pubs.acs.org/JACS

Sodorifen Biosynthesis in the Rhizobacterium *Serratia plymuthica* Involves Methylation and Cyclization of MEP-Derived Farnesyl Pyrophosphate by a SAM-Dependent *C*-Methyltransferase

Stephan von Reuss,*[,†,‡] Dajana Domik,[§] Marie Chantal Lemfack,[§] Nancy Magnus,[§] Marco Kai,[‡,§] Teresa Weise,[§] and Birgit Piechulla*[,§]

[†]Laboratory for Bioanalytical Chemistry, Institute of Chemistry, University of Neuchatel, Avenue de Bellevaux 51, CH-2000 Neuchâtel, Switzerland

[‡]Department of Bioorganic Chemistry, Max Planck Institute for Chemical Ecology, Hans-Knoell-Straße 8, D-07745 Jena, Germany

[§]Institute for Biological Sciences, University of Rostock, Albert-Einstein-Straße 3, D-18059 Rostock, Germany

Supporting Information

ABSTRACT: The rhizobacterium *Serratia plymuthica* 4Rx13 releases a unique polymethylated hydrocarbon ($C_{16}H_{26}$) with a bicyclo[3.2.1]octadiene skeleton called sodorifen. Sodorifen production depends on a gene cluster carrying a *C*-methyltransferase and a terpene cyclase along with two enzymes of the 2-*C*-methyl-D-erythritol 4-phosphate (MEP) pathway of isoprenoid biosynthesis. Comparative analysis of wild-type and mutant volatile organic compound profiles revealed a *C*-methyltransferase-dependent C_{16} alcohol called pre-sodorifen, the production of which is upregulated in the terpene cyclase mutant. The monocyclic structure of this putative intermediate in sodorifen biosynthesis was identified by NMR spectroscopy. *In vitro* assays with the heterologously expressed *S. plymuthica* *C*-methyltransferase and terpene cyclase demonstrated that these enzymes act sequentially to convert farnesyl pyrophosphate (FPP) into sodorifen via a pre-sodorifen pyrophosphate intermediate, indicating that the *S*-adenosyl methionine (SAM)-dependent *C*-methyltransferase from *S. plymuthica* exhibits unprecedented cyclase activity. *In vivo* incorporation experiments with ^{13}C-labeled succinate, L-alanine, and L-methionine confirmed a MEP pathway to FPP via the canonical glyceraldehyde-3-phosphate and pyruvate, as well as its SAM-dependent methylation in pre-sodorifen and sodorifen biosynthesis. $^{13}C\{^1H\}$ NMR spectroscopy facilitated the localization of ^{13}C labels and provided detailed insights into the biosynthetic pathway from FPP via pre-sodorifen pyrophosphate to sodorifen.

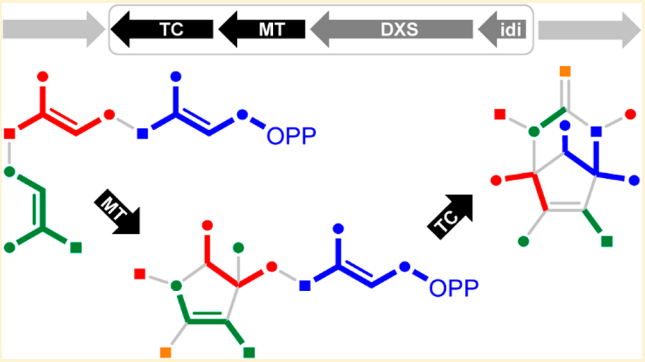

INTRODUCTION

Volatile organic compounds (VOCs) of microbial origin have been recognized as important modulators of cross-kingdom interactions.[1−7] Volatiles released by the rhizobacterium *Serratia plymuthica* 4Rx13 inhibit plant and fungal growth.[8−12] We have previously shown that *S. plymuthica* 4Rx13 releases a complex blend of volatile components that is dominated by sodorifen (**3**),[13] a polymethylated hydrocarbon ($C_{16}H_{26}$) with an unprecedented structure in which every carbon of the bicyclo[3.2.1]octadiene skeleton carries one additional methyl group (Figure 1A).[14] The extraordinary structure of sodorifen has raised considerable interest in its biogenesis and biological function. Sodorifen is exclusively produced by *S. plymuthica*, and its production varies significantly between different isolates.[15,16] Comparative transcriptomics using the sodorifen-producing *S. plymuthica* 4Rx13 strain and the nonproducing AS9 strain revealed a differentially expressed gene (SOD_c20750) that was identified as a bacterial-type terpene cyclase and shown to be essential for sodorifen production.[17] The *S. plymuthica* terpene cyclase is part of a distinct gene cluster (Figure 1B) along with a *C*-methyltransferase and two genes located at the entry and exit points of the 2-*C*-methyl-D-erythritol 4-phosphate (MEP) pathway of isoprenoid biosynthesis, a 1-deoxy-D-xylulose-5-phosphate synthase (DXS) and an isopentenyl pyrophosphate (IPP) isomerase.[18] Comparative VOC analysis of knockout mutants revealed that the terpene cyclase (TC), *C*-methyltransferase (MT), and IPP isomerase are essential for sodorifen biosynthesis. The *dxs* knockout mutant emits sodorifen at a low level, most likely due to complementation by a homologous *dxs* gene.[18] Coexpression of the *C*-methyltransferase and terpene cyclase in *E. coli* resulted in the production of small amounts of sodorifen, but none was detected upon expression of either *C*-methyltransferase and terpene cyclase alone, demonstrating that methylation of farnesyl pyrophosphate (FPP, **1a**) is a prerequisite for cyclization by the terpene cyclase.[19] Sodorifen

Received: August 8, 2018
Published: August 22, 2018

Downloaded via UNIV DE NEUCHATEL on September 19, 2018 at 11:00:47 (UTC).
See https://pubs.acs.org/sharingguidelines for options on how to legitimately share published articles.

© 2018 American Chemical Society

DOI: 10.1021/jacs.8b08510
J. Am. Chem. Soc. 2018, 140, 11855−11862

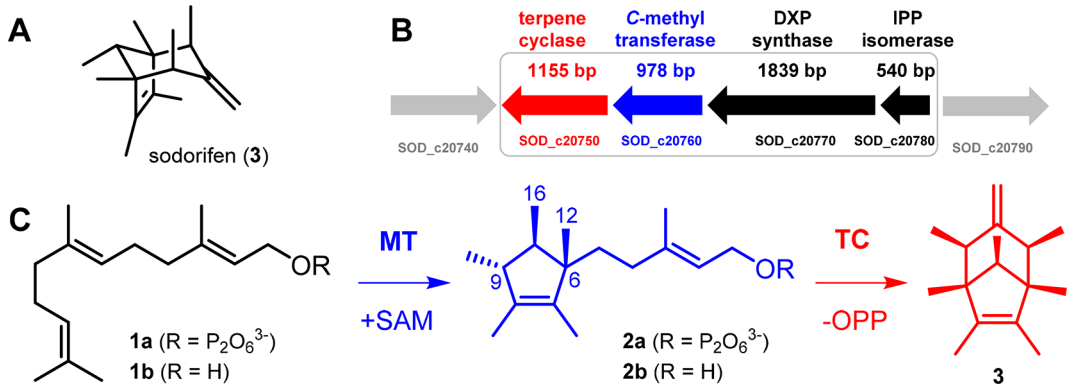

Figure 1. (A) Octamethylbicyclo[3.2.1]octadiene structure of sodorifen (**3**) from *Serratia plymuthica* 4Rx13. (B) Sodorifen gene cluster carrying the terpene cyclase (TC) and the *C*-methyltransferase (MT) along with two enzymes of the MEP pathway of terpenoid biogenesis. (C) Biosynthetic pathway starting from MEP-derived farnesyl pyrophosphate (FPP, **1a**) that is converted by the SAM-dependent *C*-methyltransferase (MT) to afford monocyclic pre-sodorifen pyrophosphate (**2a**), which serves as a noncanonical substrate for the sodorifen terpene cyclase (TC) to furnish sodorifen (**3**).

production is controlled by the carbon catabolite repression system[16] and is upregulated in *S. plymuthica* PRI-2C in response to *Fusarium culmorum* VOCs, thus suggesting a function in cross-kingdom interactions.[19]

In order to corroborate the proposed terpenoid origin of sodorifen (**3**), we studied its biogenesis using comparative analysis of wild-type and mutant VOC profiles, *in vitro* enzyme assays with the *S. plymuthica* 4Rx13 *C*-methyltransferase and terpene cyclase, and *in vivo* incorporation experiments with ^{13}C-labeled precursors. Our results highlight the importance of a *C*-methyltransferase-derived monocyclic intermediate, demonstrate that the *C*-methyltransferase exhibits unprecedented cyclase activity, confirm the involvement of a MEP-derived FPP unit plus one SAM-derived [C_1]-unit, and provide detailed insights into the complex cyclization and rearrangement reactions involved in sodorifen biosynthesis.

RESULTS AND DISCUSSION

Identification of a *C*-Methyltransferase-Dependent Intermediate in Sodorifen Biosynthesis. Comparative GC-EIMS analysis of *S. plymuthica* 4Rx13 wild-type and mutant VOCs indicated that the terpene cyclase mutant (TC::kan, kan = kanamycin resistance gene) lacks sodorifen (**3**) as well as the large diversity of isomeric C_{16} hydrocarbons (Figure 2), which confirmed the functional characterization of the terpene cyclase gene in sodorifen biosynthesis and suggested that it encodes a multiproduct terpene synthase. Furthermore, comparative GC-EIMS analysis revealed that the TC::kan mutant predominantly emits a single compound (**2b**) that is also present in trace quantities in the wild-type VOC profile. Analysis of its mass spectrum (Figure S1) supported the assumption of a sodorifen-related structure for **2b**, as indicated by a dominating fragment ion signal at *m/z* 137 $[C_{10}H_{17}]^+$ for a pentamethylcyclopentenyl moiety. The molecular formula of $C_{16}H_{28}O$ with three units of unsaturation was deduced from a molecular ion signal at *m/z* 236 $[M]^{\bullet+}$ and confirmed by ESI-HRMS (obsd *m/z* 237.2212 $[M + H]^+$, calcd for $C_{16}H_{29}O$: *m/z* 237.2213, Δ 0.3 ppm). In addition, we found that the production of **2b** strongly depends on the *C*-methyltransferase. Analysis of VOCs released by the *C*-methyltransferase mutant (MT::kan) shows none of the C_{16} components characteristic of the wild-type or terpene cyclase mutant. Instead, trace amounts of (*E*,*E*)-farnesylacetone (**4**) with *m/z* 262 $[M]^{\bullet+}$ for $C_{18}H_{30}O$ were identified based on the MS spectrum (Figure S2). These results indicate that in the absence of the *C*-methyltransferase, farnesyl pyrophosphate (C15) undergoes another extension step with an isopentenyl pyrophosphate unit to afford geranylgeranyl pyrophosphate (GGPP, C20) as a precursor to farnesylacetone (**4**).[20,21]

Aiming to elucidate the molecular structure of the *C*-methyltransferase-dependent putative intermediate in sodorifen biosynthesis, VOCs of the terpene cyclase mutant (TC::kan) that are dominated by **2b** were collected on Super-Q adsorbent, eluted with C_6D_6, and directly analyzed by NMR spectroscopy. The ^1H NMR spectrum (Figure S3) revealed one olefinic methine group at δ_H 5.42 ppm (1H, t, J = 6.6 Hz), one hydroxymethylene moiety at δ_H 3.99 ppm (2H, d, J = 6.5 Hz), three olefinic methyl groups at δ_H 1.49 ppm (3H, s), 1.50 ppm (3H, s), and 1.52 ppm (3H, s), two doublet methyl groups at δ_H 0.94 ppm (3H, d, J = 7.0 Hz) and 1.02 ppm (3H, d, J = 6.8 Hz), and one singlet methyl group at δ_H 0.79 ppm (3H, s), along with several partly overlapping multiplet signals at δ_H 1.40−2.00 ppm corresponding to six protons. The $^{13}C\{^1H\}$ NMR spectrum (Figure S4) indicated 16 carbons, including a hydroxymethylene group at δ_C 59.5 ppm and four olefinic carbons at δ_C 124.3, 134.4, 137.1, and 139.3 ppm, which implied a monocyclic structure with two double bonds. Analysis of homo- and heteronuclear coupling correlations derived from two-dimensional *dqf*-COSY, HSQC, and HMBC spectra (Figures S5−S7) indicated structure **2b** for the novel compound that we call pre-sodorifen (Figure 1C). Its relative configuration was determined by analysis of the NOESY spectrum, which displayed key NOE interactions between the singlet methyl group 12-CH_3 and the doublet methyl group 16-CH_3, as well as the allylic methine proton 9-CH (Figure S8), indicating a (6*R**,9*S**,10*S**)-configuration, as shown in Figure 1C. Although pre-sodorifen (**2b**) shares many characteristic structural features with sodorifen (**3**), such as a pentamethylcyclopentenyl moiety, it does not represent an open-chain derivative, indicating that the biosynthetic steps connecting **2b** and **3** involve the conversion of an ethylene (CH_2CH_2) bridge into a methyl-substituted methine (CH_3CH) unit. Furthermore, the observation that monocyclic pre-sodorifen (**2b**) is produced by the terpene cyclase knockout mutant (TC::kan) along with the fact that its allyl alcohol moiety is fully intact implies that it originates from an FPP-derived C_{16} precursor via nontraditional terpene cyclase activity.

DOI: 10.1021/jacs.8b08510
J. Am. Chem. Soc. 2018, 140, 11855−11862

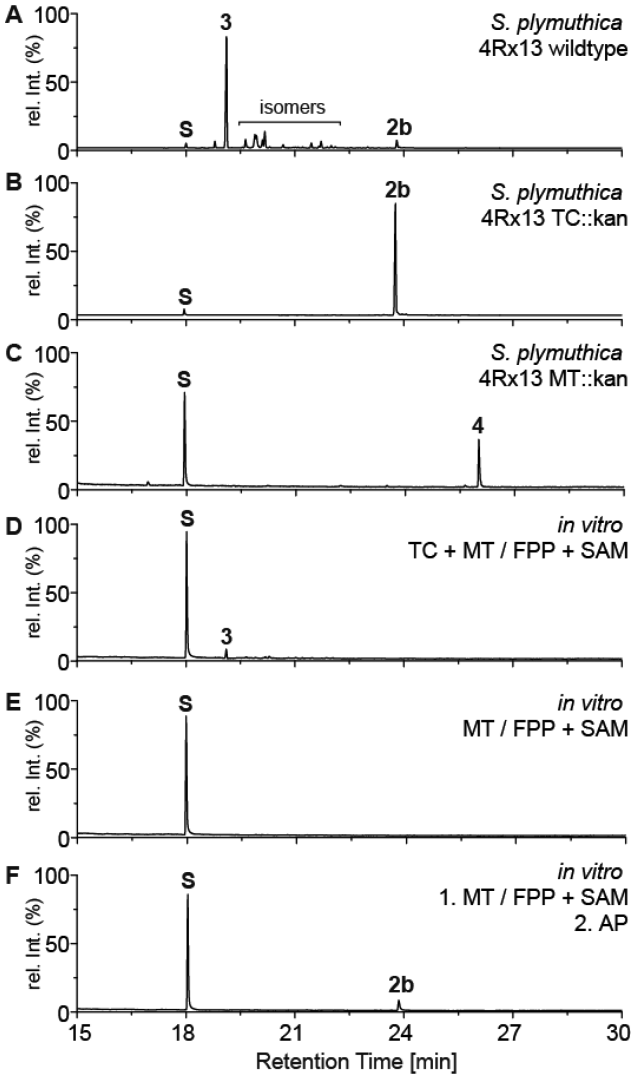

Figure 2. GC-EIMS total ion chromatograms of the *S. plymuthica* 4Rx13 VOCs from (A) wild-type, (B) the terpene cyclase knockout mutant (TC::kan), and (C) the *C*-methyltransferase knockout mutant (MT::kan). *In vitro* enzyme assays using FPP and SAM incubated with (D) the terpene cyclase (TC) and *C*-methyltransferase (MT), (E) only the MT, and (F) the MT along with alkaline phosphatase (AP). Pre-sodorifen (**2b**), sodorifen (**3**), farnesylacetone (**4**), and nonyl acetate (**S**) as internal standard at 5 ng/μL (see Figure S9 for controls).

The *S. plymuthica* *C*-methyltransferase Exhibits Unprecedented Cyclase Activity. Having identified pre-sodorifen (**2b**) as a *C*-methyltransferase-dependent putative intermediate in sodorifen biosynthesis, we studied their formation using *in vitro* enzyme assays. Incubation of the *S. plymuthica* terpene cyclase with farnesyl pyrophosphate (**1a**) in the presence or absence of *S*-adenosyl methionine (SAM) did not result in sodorifen (**3**) or any other volatile reaction product (Figure S9A,B). Furthermore, subsequent incubation with alkaline phosphatase afforded exclusively farnesol (**1b**) (Figure S9C), demonstrating that FPP (**1a**) is not a suitable substrate for the terpene cyclase. However, double enzyme assays with the *S. plymuthica* *C*-methyltransferase and terpene cyclase using FPP (**1a**) and SAM furnished sodorifen (**3**) as the sole reaction product (Figure 2D), which unambiguously established its biosynthetic origin. In addition, these results demonstrate that a *C*-methyltransferase-dependent biosynthetic intermediate derived from FPP (**1a**) serves as the precursor for sodorifen (**3**) production by the terpene cyclase. Incubation of the *S. plymuthica* *C*-methyltransferase with FPP (**1a**) and SAM did not afford any volatile reaction product (Figure 2E). However, subsequent incubation with alkaline phosphatase (AP) gave exclusively pre-sodorifen (**2b**) (Figure 2F), which implies the corresponding pyrophosphate **2a** as the *C*-methyltransferase-derived intermediate in sodorifen biosynthesis (Figure 1C).

The importance of a SAM-dependent geranyl pyrophosphate (GPP) *C*-methyltransferase acting upstream of a terpene cyclase, which accepts the noncanonical 2-methyl-GPP as a substrate, has previously been demonstrated for 2-methylisoborneol biosynthesis in cyanobacteria and *Streptomyces* sp.[22−24] Our finding that the *S. plymuthica* *C*-methyltransferase is capable of converting FPP (**1a**) into the pentamethylcyclopentenyl group containing pre-sodorifen pyrophosphate (**2a**) now demonstrates that its catalytic potential exceeds the classical SAM-dependent methyltransferase activity and includes highly uncommon cyclase activity reminiscent of the *tleD* methyltransferase involved in teleocidin B biosynthesis in *Streptomyces*.[25,26] Incubation of the *S. plymuthica* *C*-methyltransferase with FPP (**1a**) in the absence of SAM did not result in any cyclization product, and farnesol (**1b**) was observed upon co-incubation with alkaline phosphatase (Figure S9D), indicating that the SAM-dependent methylation step precedes and potentially initiates the cyclization sequence.

Succinate and L-Alanine Constitute Preferred Substrates for Sodorifen Production. Having shown that sodorifen biosynthesis involves farnesyl pyrophosphate and *S*-adenosyl methionine as substrates for the *C*-methyltransferase and terpene cyclase, we explored the underlying biosynthetic pathway using *in vivo* incorporation experiments with stable ^{13}C isotope-labeled precursors. Comparative analysis of sodorifen production in various *S. plymuthica* wild-type strains demonstrated that 4Rx13 exceeds those of the other isolates by 15−1600-fold,[16] making it well suited for *in vivo* studies.

Preliminary incorporation experiments with [2-^{13}C]-acetate, which targeted a putative polyketide or mevalonate pathway, resulted in small levels of ^{13}C enrichment (data not shown) that remained inconclusive.[14] Feeding of D-[U-$^{13}C_6$]-glucose gave only trace amounts of sodorifen (**3**) due to catabolite repression.[16] However, in agreement with the importance of a SAM-dependent *C*-methyltransferase in sodorifen biogenesis, L-[*S*-$^{13}CH_3$]-methionine was efficiently incorporated into single labeled [^{13}C]-sodorifen (**3**), and careful analysis of the EIMS fragmentation pattern suggested that the isotope label was exclusively located outside of the pentamethylcyclopentene moiety (Figure S10).

To facilitate the localization of ^{13}C labels using NMR spectroscopy, we studied the correlation of bacterial growth and sodorifen emission of wild-type *S. plymuthica* 4Rx13 in minimal media supplemented with various carbon sources. Considering that the sodorifen gene cluster suggested the involvement of the MEP pathway of isoprenoid biosynthesis (Figure 1B), we aimed to identify suitable culture conditions for robust VOC production based on substrates that could serve as metabolically close precursors for pyruvate and glyceraldehyde 3-phosphate, the ultimate building blocks for the MEP pathway. Testing a diversity of amino acid combinations, we found that sodorifen production is strongly attenuated using most of the defined amino acid mixtures in comparison to complex medium (Figure S11). However, minimal media supplemented with a combination of L-alanine and L-methionine resulted in VOC

DOI: 10.1021/jacs.8b08510
J. Am. Chem. Soc. 2018, 140, 11855−11862

Scheme 1. Biosynthetic Pathway from L-Alanine and Succinate via MEP-Derived FPP (1a) and Pre-sodorifen Pyrophosphate (2a) to Sodorifen (3) As Deduced from the Incorporation of ^{13}C-Labeled Precursors[a]

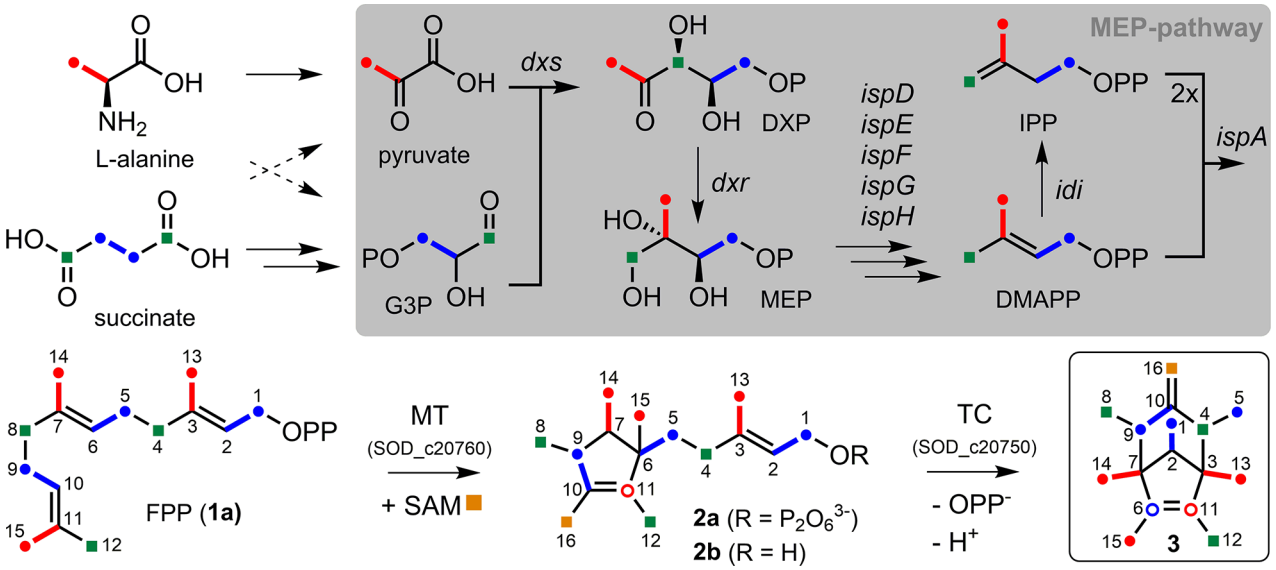

[a]Biosynthetic carbon numbering in **2a** and **3** corresponds to their position in the FPP precursor **1a**.

emission similar to those observed with nutrient broth (NB). Furthermore, we found that VOC emission was greatly enhanced using media containing succinate or fumarate as carbon source, whereas other intermediates of the tricarboxylic acid cycle were much less efficient (Figure S11). Taken together, these results indicate that minimal media supplemented with L-alanine and succinate as potential precursors for pyruvate and glyceraldehyde 3-phosphate (Scheme 1), as well as L-methionine as a precursor to SAM, could potentially be employed to study sodorifen biosynthesis in *S. plymuthica* 4Rx13.

Incorporation of ^{13}C-Labeled Precursors into Pre-sodorifen. Having identified suitable culture conditions for VOC production in *S. plymuthica*, we studied the biogenesis of pre-sodorifen (**2b**) in the terpene cyclase mutant (TC::kan) using a series of *in vivo* incorporation experiments with ^{13}C-labeled succinate, L-alanine, and L-methionine. VOCs dominated by ^{13}C-enriched pre-sodorifen (**2b**) were collected and analyzed by ^{13}C{^{1}H} NMR spectroscopy (Figure 3). Considering that pre-sodorifen biosynthesis from FPP (**1a**) depends on a SAM-dependent *C*-methyltransferase, we first determined the precise location of the additional SAM-derived [C_1]-unit by incorporation of the ^{13}C label from L-[*S*-$^{13}CH_3$]-methionine provided in a background of natural abundance L-alanine and L-threonine. Analysis of the ^{13}C{^{1}H} NMR spectrum (Figure 3B) demonstrated the highly specific incorporation into the olefinic methyl group at position 14-CH_3 of pre-sodorifen (**2b**), resulting in 75% ^{13}C enrichment as shown by ^{1}H NMR spectroscopy (Figure S12). Next, a bond labeling experiment using 20% [2,3-$^{13}C_2$]-succinate (Figure 3C) labeled five [$^{13}C_2$]-units, including [1,2-$^{13}C_2$] (d, $^{1}J_{C,C}$ = 47.5 Hz), [3,11-$^{13}C_2$] (d, $^{1}J_{C,C}$ = 41.8 Hz), [5,6-$^{13}C_2$] (d, $^{1}J_{C,C}$ = 35.9 Hz), [8,9-$^{13}C_2$] (d, $^{1}J_{C,C}$ = 40.2 Hz), and [10,16-$^{13}C_2$] (d, $^{1}J_{C,C}$ = 36.6 Hz), as shown by analysis of the direct ^{13}C,^{13}C coupling constants. In addition, three [C_1]-units at positions 7-C, 12-CH_3, and 14-CH_3 were significantly enriched with ^{13}C, indicating that one [C_2]-unit is split during the biosynthesis of **2a** from FPP (**1a**) and that the SAM-derived [C_1]-unit at 14-CH_3 is also labeled upon feeding of [2,3-$^{13}C_2$]-succinate, most likely via 5-methyl tetrahydrofolate metabolism. The remaining three carbons at positions 4-CH, 13-CH_3, and 15-CH_3 were efficiently labeled upon incorporation of 20% [1,4-^{13}C]-succinate (Figure 3D) via the glyceraldehyde 3-phosphate intermediate. To unambiguously establish the orientation of the pyruvate and glyceraldehyde-derived [C_2]-units within the pre-sodorifen skeleton, an incorporation experiment with 20% L-[3-^{13}C]-alanine was performed (Figure 3E), which labeled seven positions, five of which were part of the [C_2]-units previously labeled by [2,3-$^{13}C_2$]-succinate, including 1-C, 5-C, 9-CH, 11-CH_2, and 16-CH_3. Furthermore, L-[3-^{13}C]-alanine labeled the 12-CH_3 and 14-CH_3 position, which were also [$^{13}C_1$] enriched by [2,3-$^{13}C_2$]-succinate]. Taken together, these results confirm a terpenoid origin of pre-sodorifen (**2b**) via three MEP-derived [C_5]-isoprene units plus one SAM-derived [C_1]-unit introduced by the *C*-methyltransferase.

Incorporation of ^{13}C-Labeled Precursors into Sodorifen. Having demonstrated that ^{13}C-labeled succinate, L-alanine, and L-methionine are highly suitable to trace terpenoid metabolism via the MEP pathway in the terpene cyclase mutant (TC::kan), we studied the incorporation of these precursors into sodorifen (**3**) in wild-type *S. plymuthica* 4Rx13 (Figure 4). Although the C_s-symmetry renders it impossible to unambiguously assign the precise location and relative positions of ^{13}C labels within the sodorifen structure, we found that the superposition of isotope locations in symmetric **3** and its nonsymmetric biosynthetic precursor **2b** facilitated the assignment of all ^{13}C labels within the sodorifen (**3**) skeleton (Scheme 1).

First, the location of the SAM-derived [C_1]-unit in the sodorifen structure was unambiguously established by feeding of L-[*S*-$^{13}CH_3$]-methionine provided in a background of natural abundance L-alanine and L-threonine. VOC analysis by ^{13}C{^{1}H} NMR spectroscopy demonstrated the highly specific incorporation of ^{13}C from L-[*S*-$^{13}CH_3$]-methionine into the exocyclic methylene group at position 11-CH_2 of sodorifen (**3**) (Figure 4B), resulting in 79% ^{13}C enrichment as shown by ^{1}H NMR spectroscopy (Figure S13), in agreement with our preliminary

DOI: 10.1021/jacs.8b08510
J. Am. Chem. Soc. 2018, 140, 11855−11862

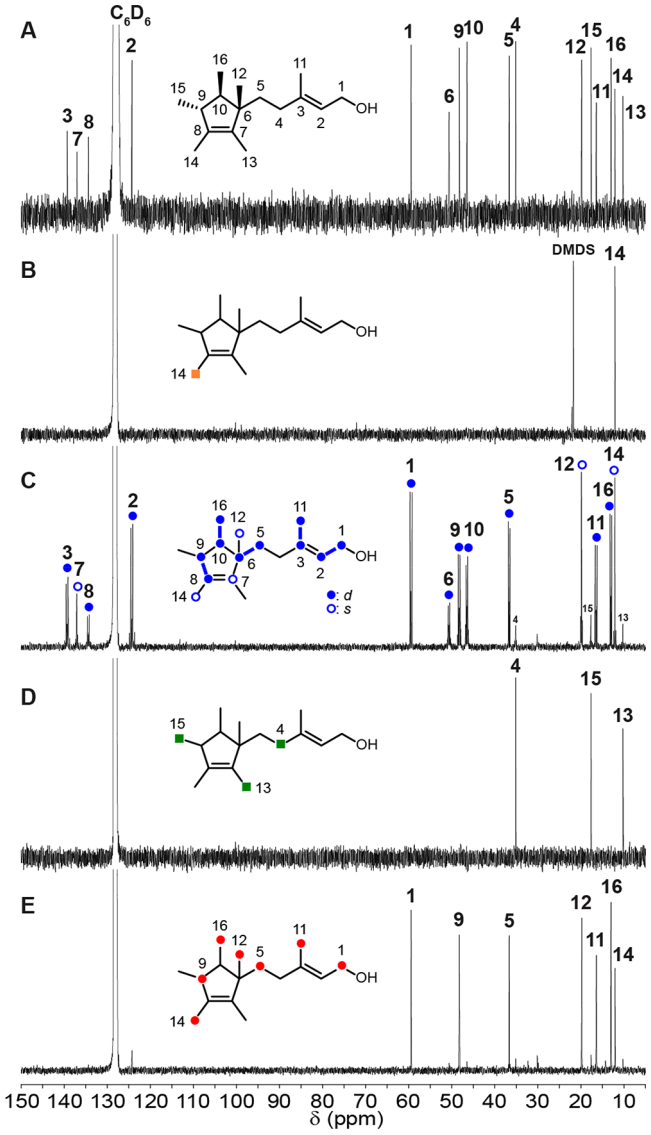

Figure 3. 100 MHz $^{13}C\{^{1}H\}$ NMR spectra of VOCs (in C_6D_6) released by the *Serratia plymuthica* 4Rx13 terpene cyclase mutant (TC::kan) showing (A) natural abundance and (B–E) ^{13}C enriched pre-sodorifen (**2b**) from incorporation of (B) L-[*S*-$^{13}CH_3$]-methionine, (C) [2,3-$^{13}C_2$]-succinate, (D) [1,4-^{13}C]-succinate, and (E) L-[3-^{13}C]-alanine. DMDS: dimethyldisulfide.

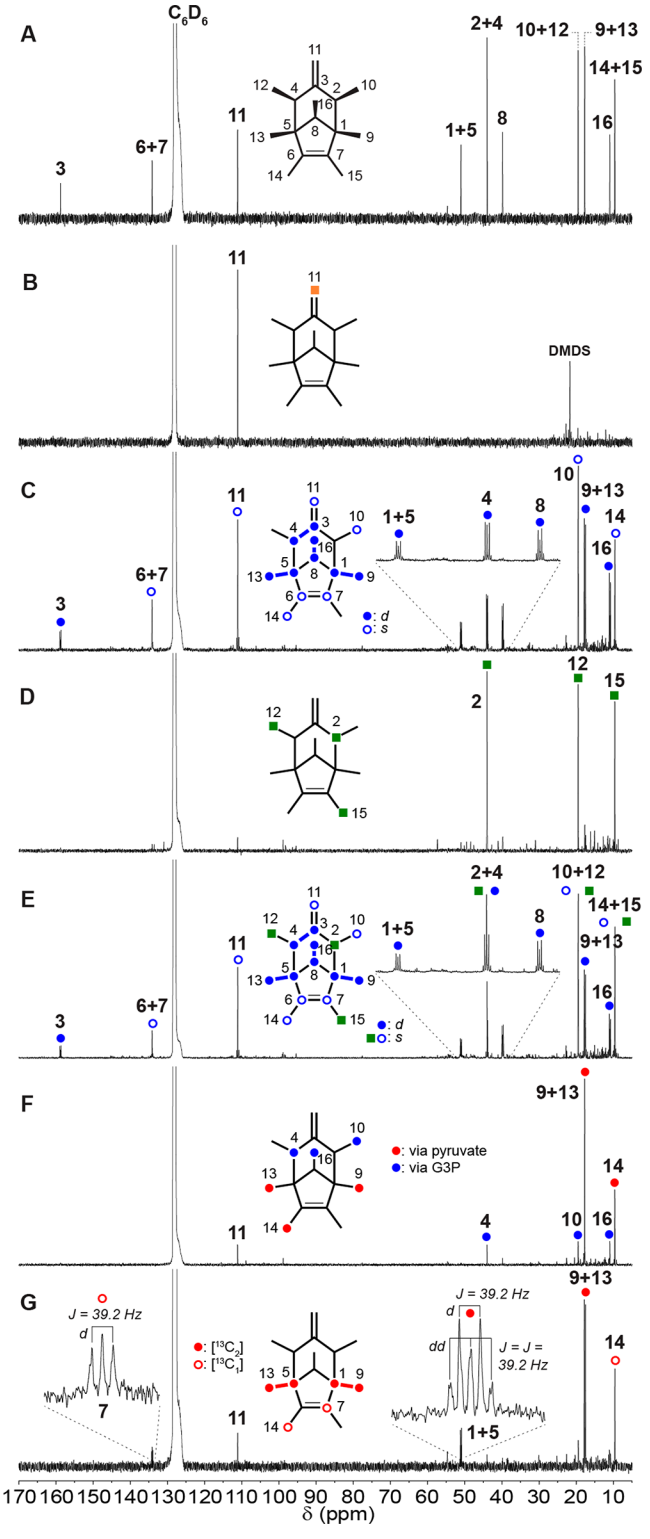

Figure 4. 100 MHz $^{13}C\{^{1}H\}$ NMR spectra of *Serratia plymuthica* 4Rx13 wild-type VOCs in C_6D_6. (A) Natural abundance and (B–G) ^{13}C-enriched sodorifen (**3**) from incorporation of (B) L-[*S*-$^{13}CH_3$]-methionine, (C) [2,3-$^{13}C_2$]-succinate, (D) [1,4-^{13}C]-succinate, (E) [U-$^{13}C_4$]-succinate, (F) L-[3-^{13}C]-alanine, and (G) L-[2,3-$^{13}C_2$]-alanine. DMDS: dimethyldisulfide.

results based on analysis of EIMS fragmentation (Figure S10). The unexpected finding that the SAM-derived [C_1]-unit contributes to different moieties within the pre-sodorifen (**2b**) (Figure 3B) and sodorifen (**3**) (Figure 4B) skeletons implies that their structural similarity, especially the presence of the peculiar pentamethylcyclopentene moiety, does not correspond to a common biogenetic origin, which indicates that the conversion of **2a** to **3** must be more complex than initially anticipated.

In order to determine the location of the glyceraldehyde-3-phosphate and pyruvate-derived [C_2]-building blocks in the sodorifen (**3**) skeleton, a bond labeling experiment using 20% [2,3-$^{13}C_2$]-succinate was performed (Figure 4C), which labeled three distinguishable [C_2]-units, including both isochoric [1,9-$^{13}C_2$]- and [5,13-$^{13}C_2$]-units (d, $^{1}J_{C,C}$ = 39.1 Hz), as well as [3,4-$^{13}C_2$] (d, $^{1}J_{C,C}$ = 40.7 Hz) and [8,16-$^{13}C_2$] (d, $^{1}J_{C,C}$ = 37.4 Hz), as shown by analysis of the direct (^{1}J) ^{13}C,^{13}C-coupling constants and relative signal intensities in the $^{13}C\{^{1}H\}$ NMR spectrum. In addition, four distinguishable [C_1]-units including 10-CH_3, 11-CH_2, and 14-CH_3, as well as the olefinic 6-C and 7-C, were significantly enriched with ^{13}C, which indicated that one

DOI: 10.1021/jacs.8b08510
J. Am. Chem. Soc. 2018, 140, 11855–11862

additional [C_2]-unit is split during the biosynthesis of **3** from **2a** (although the potential [$^{13}C_2$]-labeling of the isochoric [6,7-C_2]-unit could not be unambiguously excluded at this stage due to the symmetry of sodorifen). The three remaining carbons at positions 2-CH, 12-CH_3, and 15-CH_3 were efficiently labeled by incorporation of 20% [1,4-^{13}C]-succinate (Figure 4D). The absence of any direct (^1J) ^{13}C,^{13}C-coupling indicated that the former ^{13}C labels were not adjacent to each other. However, the position of the third ^{13}C label in relation to the other two could not be unambiguously established due to the symmetry of sodorifen (**3**) and was finally deduced from superposition with pre-sodorifen (**2b**) (Scheme 1). Considering the observation that the [2,3-$^{13}C_2$]-succinate-derived [$^{13}C_2$]-unit at the 3,4-position of sodorifen (**3**) is connected to two adjacent [1,4-^{13}C]-succinate-derived [$^{13}C_1$]-units, we explored the potential presence of a complete [$^{13}C_3$]-unit by feeding of uniformly labeled 20% [U-$^{13}C_4$]-succinate. Although the succinate-derived glyceraldehyde-3-phosphate [C_3]-unit is already split upon rearrangement of 1-deoxy-D-xylulose-5-phosphate (DXP) to MEP by DXP reductoisomerase (Scheme 1), we hypothesized that subsequent rearrangement steps during sodorifen biosynthesis might result in the reassembly of the initial [C_3]-unit. However, feeding with 20% [U-$^{13}C_4$]-succinate (Figure 4E) did not result in any additional ^{13}C,^{13}C-coupling for the signals corresponding to 2-CH, 3-C, 4-CH, and 12-CH_3 (or any other signal). Instead, the resulting ^{13}C{^{1}H} NMR spectrum represents a mixture of those obtained upon incorporation of [2,3-$^{13}C_2$]-succinate (Figure 4C) and [1,4-^{13}C]-succinate (Figure 4D), demonstrating that the sodorifen structure does not contain any intact or reassembled [C_3]-units from succinate-derived glyceraldehyde 3-phosphate. These results imply that the original succinate-derived [C_3]-unit accounts for the 3,4-position along with 15-CH_3, located on opposite sides of the sodorifen structure, indicating that the conversion of pre-sodorifen pyrophosphate (**2a**) to sodorifen (**3**) involves extensive rearrangement of the entire C_{16} carbon skeleton.

To establish the orientation of [C_2]-units and distinguish the pyruvate from glyceraldehyde 3-phosphate-derived building blocks, we performed a feeding experiment with 20% L-[3-^{13}C]-alanine in a background of natural abundance succinate (Figure 4F). Integration of the ^{1}H,^{13}C-coupled satellite signals in the ^{1}H NMR spectrum (Figure S14) revealed the highly efficient ^{13}C enrichment of both isochoric singlet methyl groups 9-CH_3 and 13-CH_3 (δ_H 0.83, d, $^1J_{H,C}$ = 125 Hz, 61% ^{13}C) along with one of the olefinic methyl groups in position 14-CH_3 (δ_H 1.41, d, $^1J_{H,C}$ = 125 Hz, 31% ^{13}C), which is in agreement with the ^{13}C{^{1}H} NMR data (Figure 4F). The observed ^{13}C enrichment was significantly larger than those of the total carbon sources provided, indicating that incorporation of L-alanine into these positions is highly preferred over succinate, which facilitated their assignment as pyruvate-derived units. Furthermore, the orientation of the glyceraldehyde 3-phosphate-derived [$^{13}C_2$]-units could also be identified based on the comparative analysis of the small intensity signals in the ^{13}C{^{1}H} NMR spectrum that revealed significantly larger ^{13}C enrichment for 4-CH, 10-CH_3, and 16-CH_3 (Figure 4F).

Having identified the pyruvate-derived methyl groups, the location of the adjacent carbons was finally determined by a bond labeling experiment with 20% L-[2,3-$^{13}C_2$]-alanine in a background of natural abundance succinate (Figure 4G). NMR spectroscopy confirmed labeling of both isochoric [1,9-$^{13}C_2$]- and [5,13-$^{13}C_2$]-units (d, $^1J_{C,C}$ = 39.2 Hz). In addition, two isolated [$^{13}C_1$]-labels were observed, indicating that the third pyruvate-derived [C_2]-unit is split during sodorifen biosynthesis from FPP (**1a**), as previously shown for pre-sodorifen (**2b**) (Figure 3C). In addition to the olefinic methyl group at position 14-CH_3, the remaining [$^{13}C_1$]-label was located in the nonadjacent olefinic 7-C position, as indicated by a broad doublet signal due to ^{13}C,^{13}C-coupling with the adjacent [$^{13}C_2$]-unit along with a dd-signal for the quaternary carbons at the 1-C and 5-C positions ($^1J_{C,C}$ = $^1J_{C,C}$ = 39.2 Hz). The ^{13}C enrichment of 7-C upon feeding with L-[2,3-$^{13}C_2$]-alanine unambiguously excluded the incorporation of a [6,7-C_2]-unit upon feeding of [2,3-$^{13}C_2$]-succinate (Figure 4C) and thereby facilitated the localization of isotope labels despite the symmetry of sodorifen (**3**).

Sodorifen Biosynthesis in *Serratia plymuthica*. *In vivo* incorporation of [^{13}C]-labeled succinate, L-alanine, and L-methionine into pre-sodorifen (**2b**) (Figure 3) and sodorifen (**3**) (Figure 4) confirms a sesquiterpene origin via three MEP-derived isoprene [C_5]-units, plus one SAM-derived [C_1]-unit introduced by the *C*-methyltransferase. The location of isotope labels facilitates the identification of the 10-position in farnesyl pyrophosphate (**1a**) for the methyltransferase-catalyzed attachment of the SAM-derived methyl group (Scheme 1). Most surprisingly, however, the incorporation of ^{13}C-labeled precursors into the characteristic pentamethylcyclopentenyl moieties of pre-sodorifen (**2b**) and sodorifen (**3**) are different, which implies that the biosynthetic pathway from **2a** to **3** as catalyzed by the *S. plymuthica* terpene cyclase is more complex than initially anticipated. While the C_s-symmetry of sodorifen (**3**) initially prevented the unambiguous localization of a ^{13}C label within its carbon skeleton, superposition of isotope positions in symmetric **3** and its nonsymmetric biosynthetic precursor **2b** facilitated the precise assignment of all ^{13}C labels in sodorifen (**3**) (Scheme 1) and, thus, provides detailed insights into sodorifen biosynthesis. Our results indicate that transformation of pre-sodorifen pyrophosphate (**2a**) to sodorifen (**3**) includes a combination of three bond-forming (2-C/7-C, 3-C/11-C, 4-C/10-C) and two bond-breaking (5-C/6-C, 10-C/11-C) events, which include the generation of a methyl-substituted methine moiety in **3** from the ethylene bridge in **2a**. On the basis of these results we propose a two-step biogenetic pathway from FPP (**1a**) to sodorifen (**3**), as shown in Schemes 2 and 3.

The biosynthesis of pre-sodorifen pyrophosphate (**2a**) from farnesyl pyrophosphate (**1a**) is catalyzed by the *S. plymuthica C*-

Scheme 2. *C*-Methyltransferase (Sp FPPMT)-Catalyzed Biosynthetic Pathway from FPP (1a) to Pre-sodorifen Pyrophosphate (2a) As Deduced from the Incorporation of ^{13}C-Labeled Precursors into Pre-sodorifen (2b)

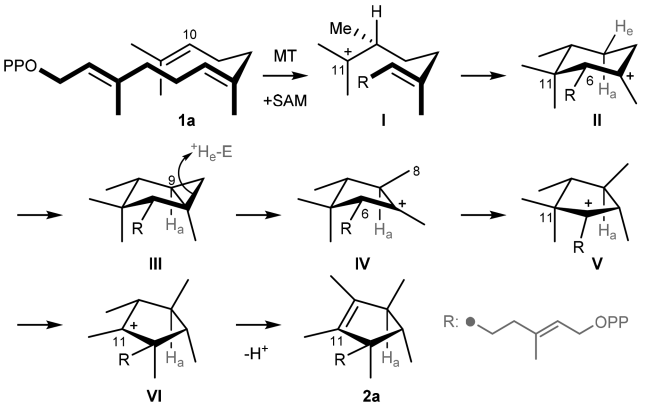

DOI: 10.1021/jacs.8b08510
J. Am. Chem. Soc. 2018, 140, 11855−11862

Scheme 3. Proposed Biosynthetic Pathway from Pre-sodorifen Pyrophosphate (2a) to Sodorifen (3) Catalyzed by the *Serratia plymuthica* Sodorifen Synthase (Sp SODS) As Deduced from the Incorporation of ^{13}C-Labeled Precursors

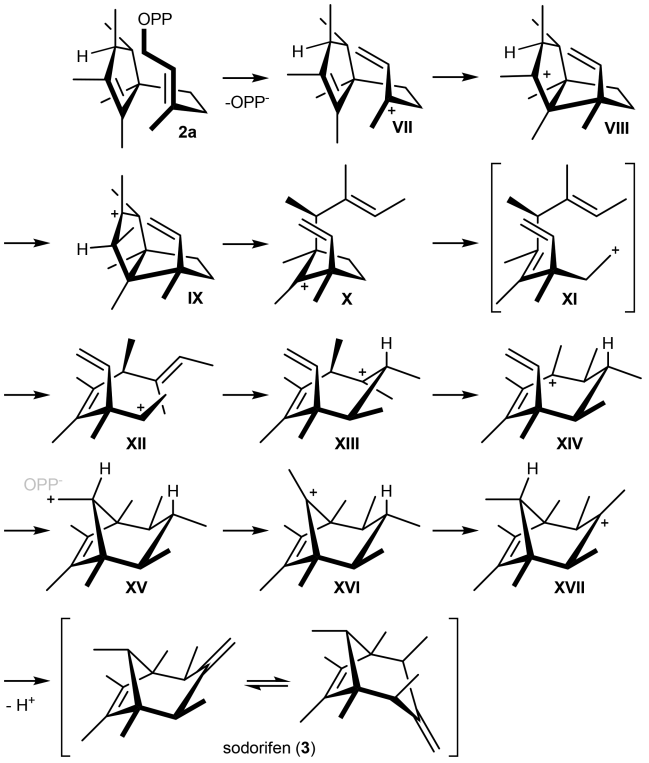

methyltransferase (called Sp FPPMT, SOD_c20760) (Scheme 2) and initiated by the electrophilic attack of a SAM-derived methyl unit at the 10-position of FPP (**1a**). Instead of a subsequent deprotonation step to afford 10-methylfarnesyl pyrophosphate, however, the tertiary carbocation at 11-C in **I** attacks the double bond at 6-C to yield carbocation **II** upon cyclization. The corresponding *O*-mannitol ether called chalmicrin has previously been identified from the fungus *Chalara microspora*[27] and *Nectria* sp.[28] Similar cyclization mechanisms have also been postulated for the biosynthesis of cyclic botryococcenes in the green microalga *Botryococcus braunii*[29−31] and the cycloiridials as precursors to odoriferous irones in *Iris* rhizomes,[32,33] indicating that *C*-methyltransferase-catalyzed cyclizations occur in diverse organisms. In *Serratia plymuthica* 4Rx13, however, the intermediate cyclohexyl carbocation **II** does not deprotonate but undergoes an additional ring contraction step that might proceed via a cyclopropyl intermediate **III** (although alternative pathways via a key 1,3-H-shift (Figure S15) or a series of multiple 1,2-H- and 1,2-Me-shifts (Figure S16) cannot be excluded). Ring opening of **III** upon reprotonation affords the cyclopentylcation **IV**, which undergoes a 1,2-H-shift to **V**, followed by a 1,2-Me-shift to **VI**, which finally affords pre-sodorifen pyrophosphate (**2a**) upon proton abstraction. The resulting pre-sodorifen pyrophosphate (**2a**) serves as the substrate for the subsequent terpene cyclase-catalyzed conversion to sodorifen (**3**) or hydrolysis of the pyrophosphate moiety to furnish pre-sodorifen (**2b**).

Considering that terpene cyclase-mediated reactions are commonly initiated by cleavage of the pyrophosphate unit, a hypothetical biosynthetic pathway from pre-sodorifen pyrophosphate (**2a**) to sodorifen (**3**) as catalyzed by the terpene cyclase (called Sp SODS, SOD_c20750) could be postulated, as shown in Scheme 3. Initial cyclization of the carbocation **VII** furnishes a bicyclo[3.3.0]octane skeleton (**VIII**) that undergoes a 1,2-H-shift to **IX**. A series of two C,C-bond cleavages along with a concerted 1,2-H-shift gives rise to **XII**, which cyclizes to furnish the monocyclic **XIII**. Following a subsequent 1,2-H-shift to **XIV**, a second cyclization step provides the bicyclo[3.2.1]-octane cation **XV**, which might be stabilized by the proximity of the pyrophosphate anion. Cation **XV** undergoes a 1,2-H-shift to **XVI** followed by a long-range H-shift to give **XVII**, which is finally deprotonated to furnish sodorifen (**3**).

CONCLUSION

Among the large diversity of volatile organic compounds released by microorganisms, the C_{16} hydrocarbon sodorifen (**3**) is exceptional given that its polymethylated bicyclo[3.2.1]-octadiene structure does not permit any immediate conclusion regarding its potential biogenesis.[14] While the ecological function of sodorifen emission by the rhizobacterium *S. plymuthica* remains enigmatic, a gene cluster including a terpene cyclase implicated in sodorifen biosynthesis has recently been identified,[17,18] the expression of which is induced in response to fungal VOCs.[19]

Using a combination of comparative GC-EIMS and NMR analysis, *in vitro* enzyme assays, and *in vivo* incorporation experiments we demonstrate that sodorifen (**3**) belongs to the family of homoterpenes, which are widely distributed in various classes of organisms but originate from diverse biogenetic pathways. For example, upon herbivore attack a large number of angiosperms produce the parasitoid and predator attracting alicyclic homoterpenes 4,8-dimethylnona-1,3,7-triene (DMNT) and 4,8,12-trimethyltrideca-1,3,7,11-tetraene (TMTT) via two enzymatic steps: the terpene synthase-catalyzed formation of the tertiary sesquiterpene (C_{15}) or diterpene (C_{20}) alcohols, (*E*)-nerolidol, and (*E*,*E*)-geranyl linalool, respectively, followed by their subsequent oxidative degradation by a single cytochrome P450 monooxygenase.[34] Insects, however, produce homoterpenoids such as the juvenile hormones JH-I and JH-II, which are known to originate from incorporation of propionate via homomevalonate intermediates.[35−37] Several biosynthetically related alicylic homofarnesene derivatives have been described from ants,[38] and cyclic homosesquiterpenes including 3-methyl-α-himachalene and 9-methylgermacrene B are known as sandfly pheromones.[39] In bacteria the production of the homoterpene 2-methylisoborneol is widespread in *Streptomyces* species and known to proceed via a terpene synthase-catalyzed cyclization of a noncanonical 2-methylgeranyl pyrophosphate intermediate, derived from SAM-dependent 2-methylation of geranyl pyrophosphate.[22−24] Our results now demonstrate that the biogenesis of the C16 homoterpene sodorifen (**3**) in *S. plymuthica* proceeds via a related pathway including the terpene cyclase-catalyzed transformation of monocyclic pre-sodorifen pyrophosphate (**2a**). This highly uncommon intermediate is generated by the formal 10-methylation of farnesyl pyrophosphate (**1a**) by the SAM-dependent *C*-methyltransferase, which exhibits unprecedented cyclase activity reminiscent of the *tleD* methyltransferase involved in teleocidin B biosynthesis in *Streptomyces*.[25,26] *In vivo* incorporation experiments and localization of ^{13}C labels by NMR spectroscopy confirmed a biogenetic pathway via MEP-derived FPP (**1a**) plus a methionine-derived [C_1]-unit introduced by the *C*-methyltransferase. Comparative analysis of isotope locations further revealed that conversion of pre-sodorifen (**2a**) as catalyzed by

DOI: 10.1021/jacs.8b08510
J. Am. Chem. Soc. 2018, 140, 11855−11862

the terpene cyclase involves extensive rearrangement of the entire carbon skeleton including several bond-breaking reactions, thus providing detailed insights into the biogenesis of sodorifen (**3**). Based on these results putative biogenetic pathways could be proposed, but alternative scenarios are also conceivable. Additional experiments using specifically ^{2}H-labeled substrates will be required to unambiguously establish the various hydride shifts involved, whereas molecular modeling and site-directed mutagenesis will reveal how various amino acid residues within the active site of the *S. plymuthica* *C*-methyltransferase and terpene cyclase guide the elaborate rearrangement mechanism that converts MEP-derived FPP (**1a**) via monocyclic pre-sodorifen pyrophosphate (**2a**) into sodorifen (**3**).

METHODS

Detailed procedures for cultivation of *S. plymuthica* 4Rx13, VOC collection and analysis, *in vitro* enzyme assays, and *in vivo* feeding experiments are provided in the Supporting Information.

ASSOCIATED CONTENT

Supporting Information

The Supporting Information is available free of charge on the ACS Publications website at DOI: 10.1021/jacs.8b08510.

Experimental procedures, spectroscopic data, and supporting figures as indicated in the main text (PDF)

AUTHOR INFORMATION

Corresponding Authors

*stephan.vonreuss@unine.ch

*birgit.piechulla@uni-rostock.de

ORCID

Stephan von Reuss: 0000-0003-4325-5495

Notes

The authors declare no competing financial interest.

ACKNOWLEDGMENTS

Support by the Deutsche Forschungsgemeinschaft (DFG) (Pi153/28-1 and 36-1), the University of Rostock, the Max Planck Society (MPG), the University of Neuchatel (UniNE), and the Swiss National Science Foundation (SNSF) is gratefully acknowledged. We thank Claudia Dinse and Dörte Warber for technical assistance

REFERENCES

(1) Schulz-Bohm, K.; Martin-Sánchez, L.; Garbeva, P. *Front. Microbiol.* **2017**, *8*, 02484.

(2) Effmert, U.; Kalderas, J.; Warnke, R.; Piechulla, B. *J. Chem. Ecol.* **2012**, *38*, 665−703.

(3) Sharifi, R.; Ryu, C. M. *Front. Microbiol.* **2016**, *7*, 196.

(4) Wenke, K.; Kai, M.; Piechulla, B. *Planta* **2010**, *231*, 499−506.

(5) Werner, S.; Polle, A.; Brinkmann, N. *Appl. Microbiol. Biotechnol.* **2016**, *100*, 8651−8665.

(6) Piechulla, B.; Lemfack, M. C.; Kai, M. *Plant, Cell Environ.* **2017**, *40*, 2042−2067.

(7) Piechulla, B.; Degenhardt, J. *Plant, Cell Environ.* **2014**, *37*, 811−812.

(8) Vespermann, A.; Kai, M.; Piechulla, B. *Appl. Environ. Microbiol.* **2007**, *73*, 5639−5641.

(9) Kai, M.; Effmert, U.; Berg, G.; Piechulla, B. *Arch. Microbiol.* **2007**, *187*, 351−360.

(10) Kai, M.; Vespermann, A.; Piechulla, B. *Plant Signaling Behav.* **2008**, *3*, 482−484.

(11) Kai, M.; Piechulla, B. *FEBS Lett.* **2009**, *583*, 3473−3477.

(12) Kai, M.; Piechulla, B. *Plant Signaling Behav.* **2010**, *5*, 444−446.

(13) Kai, M.; Crespo, E.; Cristescu, S. M.; Harren, F. J. M.; Francke, W.; Piechulla, B. *Appl. Microbiol. Biotechnol.* **2010**, *88*, 965−976.

(14) von Reuß, S. H.; Kai, M.; Piechulla, B.; Francke, W. *Angew. Chem., Int. Ed.* **2010**, *49*, 2009−2010.

(15) Weise, T.; Thürmer, A.; Brady, S.; Kai, M.; Daniel, R.; Gottschalk, G.; Piechulla, B. *FEMS Microbiol. Lett.* **2014**, *352*, 45−53.

(16) Magnus, N.; Weise, T.; Piechulla, B. *Front. Microbiol.* **2017**, *8*, 2522.

(17) Domik, D.; Thürmer, A.; Weise, T.; Brandt, W.; Daniel, R.; Piechulla, B. *Front. Microbiol.* **2016**, *7*, 737.

(18) Domik, D.; Magnus, N.; Piechulla, B. *FEMS Microbiol. Lett.* **2016**, *363*, fnw139.

(19) Schmidt, R.; Jager, V.; Zühlke, D.; Wolff, C.; Bernhardt, J.; Cankar, K.; Beekwilder, J.; Ijcken, W. V.; Sleutels, F.; Boer, W.; Riedel, K.; Garbeva, P. *Sci. Rep.* **2017**, *7*, 862.

(20) Ferezou, J. P.; Barbier, M.; Berreur-Bonnenfant, J. *Helv. Chim. Acta* **1978**, *61*, 669−674.

(21) Boland, W.; Gäbler, A.; Gilbert, M.; Feng, Z. *Tetrahedron* **1998**, *54*, 14725−14736.

(22) Giglio, S.; Chou, W. K. W.; Ikeda, H.; Cane, D. E.; Monis, P. T. *Environ. Sci. Technol.* **2011**, *45*, 992−998.

(23) Brock, N. L.; Ravella, S. R.; Schulz, S.; Dickschat, J. S. *Angew. Chem., Int. Ed.* **2013**, *52*, 2100−2104.

(24) Komatsu, M.; Tsuda, M.; Omura, S.; Oikawa, H.; Ikeda, H. *Proc. Natl. Acad. Sci. U. S. A.* **2008**, *105*, 7422−7427.

(25) Awakawa, T.; Zhang, L.; Wakimoto, T.; Hoshino, S.; Mori, T.; Ito, T.; Ishikawa, J.; Tanner, M. E.; Abe, I. *J. Am. Chem. Soc.* **2014**, *136*, 9910−9913.

(26) Yu, F.; Li, M.; Xu, C.; Sun, B.; Zhou, H.; Wang, Z.; Xu, Q.; Xie, M.; Zuo, G.; Huang, P.; Guo, H.; Wang, Q.; He, J. *Biochem. J.* **2016**, *473*, 4385−4397.

(27) Fex, T. *Phytochemistry* **1982**, *21*, 367−369.

(28) Wang, R.-S.; Gong, T.; Zhu, P.; Cheng, K.-D. *J. Chin. Pharm. Sci.* **2012**, *21*, 183−186.

(29) de Mesmay, R.; Metzger, P.; Grossi, V.; Derenne, S. *Org. Geochem.* **2008**, *39*, 879−893.

(30) Huang, Z.; Poulter, C. D. *J. Org. Chem.* **1988**, *53*, 4089−4094.

(31) Metzger, P.; Largeau, C. *Appl. Microbiol. Biotechnol.* **2005**, *66*, 486−496.

(32) Marner, F.-J.; Gladtke, D.; Jaenicke, L. *Helv. Chim. Acta* **1988**, *71*, 1331−1338.

(33) Marner, F.-J. *Curr. Org. Chem.* **1997**, *1*, 153−186.

(34) Tholl, D.; Sohrabi, R.; Huh, J. H.; Lee, S. *Phytochemistry* **2011**, *72*, 1635−1646.

(35) Morgan, E. D.; Wilson, I. D. *Comprehensive Natural Products Chemistry* **1999**, *8*, 263−375.

(36) Schooley, D. A.; Judy, K. J.; Bergot, B. J.; Hall, M. S.; Siddall, J. B. *Proc. Natl. Acad. Sci. U. S. A.* **1973**, *70*, 2921−2925.

(37) Peter, M. G.; Dahm, K. H. *Helv. Chim. Acta* **1975**, *58*, 1037−1048.

(38) Morgan, E. D. *Physiol. Entomol.* **2009**, *34*, 1−17.

(39) Hamilton, J. G. C. *Parasite* **2008**, *15*, 252−256.

DOI: 10.1021/jacs.8b08510
J. Am. Chem. Soc. 2018, 140, 11855−11862